ACADEMIA ROMÂNĂ
Revue Roumaine de Chimie
https://www.icf.ro/rrch/

Rev. Roum. Chim.,
2024, *69*(1–2), 5–17
DOI: 10.33224/rrch.2024.69.1-2.01

Papers

PREDICTION OF SOME PHYSICAL PROPERTIES OF NANOFLUIDS INCLUDING VARIOUS METAL OXIDES USING ARTIFICIAL NEURAL NETWORK

Behrouz RAEI[a,*] and Alireza BOZORGIAN[b]

[a]Department of Chemical Engineering, Mahshahr Branch, Islamic Azad University, Mahshahr, Iran,
e-mail: behrouz.raei@iau.ac.ir
[b]Department of Chemical Engineering, Mahshahr Branch, Islamic Azad University, Mahshahr, Iran,
e-mail: alireza.bozorgian@iau.ac.ir

Received June 25, 2022

In this study, physical properties of nanofluids such as viscosity and thermal conductivity are investigated. Although there are many experimental and theoretical correlations and models available to predict these parameters, predictions are highly conflicting because the involved mechanisms are not fully understood. For instance, the predicted values of dynamic viscosity of γ-Al_2O_3/water nanofluids (at a volume fraction of 0.001) by different models range between 0.0005623 and 0.0403 kg/m.s and thermal conductivity ranges within 0.866 and 1.551 W/m·K under the same conditions. In this work, 184 experimental data of thermophysical properties of various metal oxide nanoparticle including Al_2O_3, SiO_2, TiO_2, Fe_2O_3, MgO, and CuO at a temperature range of 30 to 65 ºC, diameter range of 10 to 50 nm, and volume fraction between 0.004% to 2% were collected from various publications. In this work, artificial neural network (ANN) has been implemented. The parameters of thermal conductivity and dynamic viscosity have been correlated to nanofluid concentration, temperature, particle size and molecular weight. It has been found that the topography of (4, 4, 4) from the ANN provides about 2% and 1% cross-validating and testing error respectively. Additionally, a sensitivity analysis was performed and the effect of individual parameters was analyzed.

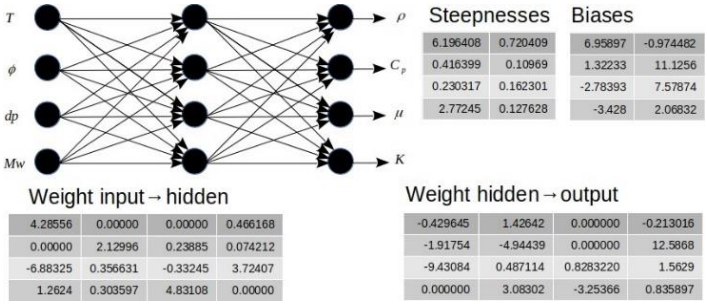

INTRODUCTION

A nanofluid is a fluid containing nanometer-sized particles, called nanoparticles. These fluids are engineered colloidal suspensions of nanoparticles in a base fluid. The nanoparticles used in nanofluids are typically made of metals, oxides, carbides, or carbon nanotubes. Common base fluids include water, ethylene glycol and oil.[1] Nanofluids are determined as nanoparticles' dilute suspensions with sizes less than 100 nm. The order of magnitude of thermal conductivity of the nonmetallic or metallic nanoparticles including CuO, Al_2O_3, Cu, TiO_2, and SiO_2 are often higher compared to the conventional fluid. These nanofluids, compared to the conventional solid-

* Corresponding author: behrouz.raei@iau.ac.ir

mixtures, contain superior properties such as minimal clogging in flow passage, higher thermal conductivity,[2] reduced pumping power, long-term homogeneity, and stability. Therefore, it is necessary to enhance various potential uses of nanofluids such as their heat transfer rate. The heat transfer and pressure drop characteristics of nanofluids are defined by the relative difference in the nanofluids'thermophysical properties like thermal conductivity, viscosity, specific heat, and density. Thermal conductivity contributes significantly to the determination of the nanofluids' thermal efficiency. It is taken into account as a function of multiple factors such as particle morphology (shape and size), material, concentration, base fluid properties, pH value, additives, and fluid temperature. Although optimizing thermal conductivity is the main prospect of adding nanoparticles to the base fluid, the mentioned property is not the only property affecting nanofluids hydrothermal performance. Another potential property of nanofluids is viscosity, which characterizes pressure drop and convective heat transfer rate. The factors that influence the nanoparticles' viscosity are shear rate, temperature, particle morphology, concentration, and surfactants.[3]

Various theoretical and experimental investigations exist in the literature on modeling nanofluid thermal conductivity and viscosity. According to the published results, there is no consistency between the mechanisms for heat transfer improvement or a unified possible description for the relatively large differences in the findings even for the same nanoparticle size and base fluid. Presently, no theoretical results with acceptable accuracy exist in the literature for forecasting nanofluid thermal conductivity and also viscosity.

Nanofluids' thermal conductivity and viscosity are influenced by multiple factors. As a result, using classic Maxwell,[4] Hamilton and Crosser (HC),[5] and Wasp models[6] for thermal conductivity estimation and viscosity of nanofluids provide rather unreliable results. The main reason for such uncertainty is that these models only integrate the impact of the volume concentration of the particle. Some researchers suggested their own models for estimation of the viscosity and thermal conductivity of nanofluids in terms of their experimental findings. To date, no fundamental correlations have been created for the exact prediction of the mentioned properties of nanofluids. Some main models proposed for nanofluids' thermophysical properties are provided in the next section.

THERMAL CONDUCTIVITY

Hypothetical models

The Maxwell model[4] is possibly the first model proposed for thermal conductivity (k_{nf}) of solid-liquid suspension, as follows:

$$k_{nf} = \frac{k_p + 2k_f + 2\phi\left(k_p - k_f\right)}{k_p + 2k_f - \phi\left(k_p - k_f\right)} k_f \qquad (1)$$

where k_f and k_p represent the conductivities of the base fluid and the nanoparticles, respectively. The model is developed for spherical particles with a low concentration ($\Phi \leq$ 1%).

Considering the interactions between spherical particles, the following model was proposed by Bruggeman:[7]

$$\frac{k_{nf}}{k_f} = \frac{(3\Phi - 1)\frac{k_p}{k_f} + \{3(1-\Phi) - 1\} + \sqrt{\Delta}}{4} \qquad (2)$$

where

$$\Delta = \left[(3\Phi - 1)\frac{k_p}{k_f} + \{3(1-\Phi) - 1\}\right]^2 + 8\frac{k_p}{k_f}.$$

Crosser and Hamilton [5] developed the Maxwell model by adding a shape factor to it as follows:

$$\frac{k_{nf}}{k_f} = \frac{k_p + (n-1)k_f + (n-1)\Phi\left(k_p - k_f\right)}{k_p + (n-1)k_f - \Phi\left(k_p - k_f\right)} \qquad (3)$$

where shows the experimental shape factor ($n = \frac{3}{\psi}$), where ψ represents the particle sphericity.

The sphericity parameter for spherical particles is 1, while it is 0.5 for cylindrical particles.

It is noteworthy that although the mentioned models are valid for large particle sizes, they underestimate the thermal conductivity. Nevertheless, they still are widely used in numerical simulation of nanofluids. Several attempts have been made to extend or renovate the previous models and take in consideration the phenomena involved in heat conduction of nanoparticles and nanofluids such as nanolayer, nanoparticle interaction, aggregation and Brownian motion. By dispersing the nanoparticles in a liquid, a thin liquid layer is created over the nanoparticles' surface known as the "liquid nanolayer". Choi and Yu[8] took into account this factor to propose a novel thermal conductivity model as:

$$k_{nf} = \frac{k_p + 2k_f + 2\left(k_p - k_f\right)(1+\gamma)^3\Phi}{k_p + 2k_f - 2\left(k_p - k_f\right)(1+\gamma)^3\Phi} k_f \quad (4)$$

where γ shows the ratio of liquid nanolayer thickness to the nanoparticle's radius and is generally supposed to be 0.1.

Xuan *et al.*[9] offered a model for nanofluids thermal conductivity based on the Brownian motion and aggregation of nanoparticles as follows:

$$\frac{k_{nf}}{k_f} = \frac{k_p + 2k_f - 2\Phi\left(k_f - k_p\right)}{k_p + 2k_f + \Phi\left(k_f - k_p\right)} + \frac{\rho_p \Phi c_{p,f}}{2k_f}\sqrt{\frac{2\kappa_B T_{ave}}{3\pi d_p \mu_f}} \quad (5)$$

where k_B shows the Boltzmann constant and d_p represents nanoparticle diameter (nm). Thus, according to this model, the nanofluids' thermal conductivity relies on the thermal conductivity of nanoparticles, the volume fraction of the nanoparticles, the mixture temperature, the nanoparticles' size, and the base fluid properties such as viscosity, specific heat capacity, and thermal conductivity.

The following model was provided by Koo and Kleinstreuer[10] for nanofluid's thermal conductivity (K-K model):

$$K_{nf} = k_{static} + k_{Brownian} = \frac{k_p + 2k_f + 2\phi\left(k_p - k_f\right)}{k_p + 2k_f - \phi\left(k_p - k_f\right)} k_f + 5\times 10^4 \beta\Phi\rho_p c_{p,f}\sqrt{\frac{\kappa_B T}{\rho_p d_p}} f(T,\Phi) \quad (6)$$

where β and f represent the two experimental functions and k_B shows the Boltzmann constant. This model includes two dynamic and static parts.

A model was presented by Xue *et al.*[11] to obtain the thermal conductivity of nanosuspensions containing carbon nanotubes (CNTs). This model, which was built on the basis of the classic model of Maxwell, considers the influence of CNTs' physical features such as spatial distribution and axial ratio:

$$k_{nf} = \frac{1 - \Phi + 2\Phi\frac{k_p}{k_p - k_{bf}}\ln\left(k_p + k_{bf}\right)}{2k_{bf}} \Big/ \frac{1 - \Phi + 2\Phi\frac{k_{bf}}{k_p - k_{bf}}\ln\left(k_p + k_{bf}\right)}{2k_{bf}} k_{bf} \quad (7)$$

Experimental correlations

The experimental-based correlations have been mostly proposed for oxide and spherical metallic nanoparticles. Maiga et al.[12] offered a set of experimental correlations using experimental data obtained from spherical metallic and nano-oxide particles.

for Al_2O_3/water:

$$k_{nf} = (4.97\Phi^2 + 2.72\Phi + 1)k_f \quad (8)$$

for Al_2O_3/ ethylene glycol:

$$k_{nf} = (28.905\Phi^2 + 2.8273\Phi + 1)k_f \quad (9)$$

These correlations were provided for nanoparticles with a specific size of 28 nm. Incorporating different empirical results for nanofluids' thermal conductivity, Corcione[13] presented a correlation as:

$$\frac{k_{nf}}{k_f} = 1 + 4.4R_p^{0.4}Pr_f^{0.66}\left(\frac{T}{T_{freez}}\right)^{10}\left(\frac{k_p}{k_f}\right)^{0.03}\Phi^{0.66} \quad (10)$$

where

$$R_p = \frac{2\rho_f \kappa_B T}{\pi\mu_f^2 d_p} \quad (11)$$

This relation is valid for nanoparticle sizes within the range of 10–150 nm, temperatures of 294–324 K, and volume fractions of 0.2–9%.

A general correlation was provided by Vafai and Khanafer[14] for the thermal conductivity of CuO/water nanofluids and Al_2O_3/water as:

$$\frac{k_{nf}}{k_f} = 1 + 1.0112\Phi + 2.4375\phi\left(\frac{47}{d_p(nm)}\right) - 0.0248\Phi\left(\frac{k_p}{0.613}\right) \quad (12)$$

This correlation is developed for nanoparticle size within the range of 13–80 nm and volume fractions of over 15%. The following empirical correlation was proposed by Ho *et al.*[15] for alumina/water nanofluids' thermal conductivity with the size of nanoparticles just as 33 nm:

$$k_{nf} = k_f(1 + 2.944\Phi + 19.672\Phi^2) \quad (13)$$

The above relation is validated for volume concentrations up to 4%. Williams *et al.*[16] developed the following correlation for alumina/water nanofluids' thermal conductivity in terms of the limited experimental data:

$$k_{nf} = k_f(T)(1 + 4.5033\Phi) \quad (14)$$

Thus far, no comprehensive model has been presented for prediction of the thermal conductivity of a nanofluid, which is a major challenge in nanofluid studies.

Viscosity (μ_{nf})

Theoretical models

Einstein provided a model on the basis of the kinetic theory for mixtures of liquids and solids. This model is valid for volume fractions of less than 1%. It provides the mixture effective viscosity as[14]:

$$\mu_{nf} = \mu_f(1 + 2.5\Phi) \quad (15)$$

The following model was provided by Brinkman for particles (spherical) operational up to 4% particle volume loadings[17]:

$$\mu_{nf} = \frac{\mu_f}{(1-\Phi)^{2.5}} \quad (16)$$

Batchelor[16] provided a novel model to estimate the viscosity.

$$\frac{\mu_{nf}}{\mu_f} = (1 + 2.5\Phi + 6.5\Phi^2) \quad (17)$$

Experimental correlations

Maiga *et al.*[19] provided two experimental correlations for the viscosity of Al_2O_3-water and Al_2O_3-EG nanofluids:

$$\mu_{nf} = (123\Phi + 7.3\Phi + 1)\mu_f \quad (18)$$

$$\mu_{nf} = (306\Phi^2 - 0.19\Phi + 1)\mu_f \quad (19)$$

Based on the experimental data, Ho *et al.*[15] offered a correlation for predicting the viscosity of alumina/water nanofluids in which the nanoparticles'size is 33 nm (valid for $\Phi \leq$ 4%):

$$\mu_{nf} = \mu_f(1 + 4.93\Phi + 222.4\Phi^2) \quad (20)$$

Vajjha[20] presented a further comprehensive model for copper oxide and aluminum oxide nanoparticles dispersed in a mixture containing ethylene glycol and water (60:40 wt.%):

$$\frac{\mu_{nf}}{\mu_f} = Ae^{B\Phi} \quad (21)$$

where A = 0.983 and B = 12.959 at temperatures of 20–90°C for aluminum oxide nanoparticles and A = 0.9197 and B = 22.8539 for copper oxide nanoparticles. Williams *et al.*[16] provided the dynamic viscosity equations in terms of the in adequate experimental data for the γ-Al_2O_3/water nanofluid.

$$\mu_{\downarrow}nf = \mu_{\downarrow}f\ (T)\exp[4.91\varphi/((0.2092 - \Phi))] \quad (22)$$

Density (ρ_{nf})

For a nanofluid with a volume fraction of Φ, it is possible to calculate the nanofluid density as follows [21]:

$$\rho_{nf} = \rho_f(1-\Phi) + \rho_p\Phi \quad (23)$$

Specific heat capacity (cp,nf)

The nanofluids' specific heat capacity is determined as[14]:

$$c_{p,nf} = \frac{\rho_f c_{pf}(1-\Phi) + \rho_p c_{pp}\Phi}{\rho_{nf}} \quad (24)$$

where $c_{p,p}$, and $c_{p,f}$ respectively show the specific heat capacities of nanoparticles and base fluid. A common simplified model valid for similar nanoparticle density to the base fluid is provided as:

$$c_{pnf} = (1-\Phi)c_{pf} + \Phi c_{pp} \quad (25)$$

To validate the existing models and correlation, new experiments and calculations were performed.

These experiments and calculations include viscosity and thermal conductivity of γ-Al_2O_3/water nanofluid with the following specification: φ = 0.1%, T = 65°C, d_p = 20 nm and morphology (spherical) (Table 1). Preparation of nanofluids is the first key step in experimental studies using nanoparticles to improve the thermal efficiency of fluids. Two methods including single-step and two-step exist for nanofluid production. As the nanoparticles are commercially available; many researchers used two-step procedure for preparing nanofluids. A transmission electron microscope (TEM) was used to approximate the size of the primary nanoparticles. As shown in Fig. 1, it is clear that the primary shape of nanoparticles is approximately spherical.

In this work, SVM-3000 Anton Paar viscometer was used to measurethe viscosity of nanofluds. This device can measure the kinematic and dynamic viscosity of fluid via only 2.5 ml of the sample. Dynamic viscosity was measured by evaluating the needed force for rotating an internal cylinder. The viscometer was calibrated via toluene and isopropyl alcohol according to the instruction. Each run was repeated 3 times and the repeatability was in the order of ± 0.001 mm^2/s. The device mentioned has been used in previous studies.[22]

Also, to quantify the thermal conductivity of the nanofluds, a KD2 pro Decagon conductivity

measurement instrument probe with acuracy of 1% of reading value was used. Viscosity and thermal conductivity of nanofuids were measured as 0.000453 kg/m·s and 0.6601 W/m·K, respectively.

Table 1

Specifications of the nanoparticles

φ (Volume fraction)	Base fluid	Nanoparticle	T (°C)	d_p (nm)	Morphology
0.001	Distillate Water	γ-Al_2O_3	65	20	Spherical

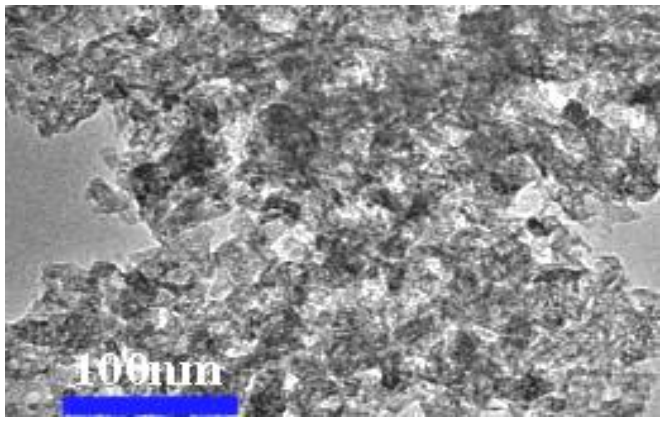

Fig. 1– Image of TEM nanoparticles used in this study.

Tables 2 and 3 respectively represent the predicted values of dynamic viscosity and thermal conductivities. The maximum deviation between predictions was nearly 80% and 200% for viscosity and thermal conductivity, respectively. As it turns out, the forecast results are very different from each other.

Recently, probing models based on experimental data, such as neural networks, fuzzy logic, and genetic programming are proposed to forecast the required data in order to avoid further experiments. This type of models can be applied to identify underlying complex relationships by data mining approach with noisy and lacking data. Kurt and Kayfeci[23] suggested an artificial neural network (ANN) model to anticipate the thermal conductivity of ethylene glycol/water-based nanofluids by taking into account temperature, volume fraction and density of nanoparticles. Papari *et al.*[24] planned a model for predicting thermal conductivity of single-wall carbon nanotubes and multi-walled carbon nanotubes using a diffusion neural network. Alirezaei *et al.*[25] considered the rheological behavior of the MWCNT-MgO (10–90%) hybrid nanofluid (oil-based) at different volumetric fractions, temperatures, and shear rates. They provided a three-variable correlation to figure out experimental data and then used artificial neural networks to model their experimental results. Hojjat *et al.*[26] used a three-layer feed-forward neural network to model the thermal conductivity of γ-Al_2O_3,TiO_2 and CuO nanopartcles in a CMC aqueous solution. The effects of CuO nanoparticles mass fraction and temperature was investigated on the dynamic viscosity and thermal conductivity of CuO/viscous paraffin nanofluid by Karimipour *et al.*[27] Two separated correlation including temperature and mass fraction of CuO nanoparticle was predicted by using hybrid GMDH-type neural network method for estimating relative dynamic viscosity and thermal conductivity of nanofluid. Longo *et al.*[28] present an Artificial Neural Network (ANN) model for predicting the dynamic viscosity of oxide nanoparticles suspension in water and ethylene glycol. The model accounts for the effect of temperature, nanoparticle volume fraction, nanoparticle diameter, cluster of nanoparticles average size, and base fluid properties. The model shows a fair agreement in predicting experimental data: the mean absolute percentage error (MAPE) is 4.15%. Thermal conductivity of ZnO–EG using experimental data and ANN method has been carried out by Hemmat Esfe *et al.*[29] Predicting the viscosity of graphene nanoplatelets nanofluid with the help of multi-layered perceptron artificial neural network and genetic algorithm was the main aim of Vakili *et al.*[30] research. Genetic algorithm in artificial neural network is used to boost the learning process. In case of comparison the results display that the given model which is the combination of genetic algorithm and artificial

neural network is consistent with experimental work. Shi *et al*.[31] studied to predict the thermophysical properties of magnetic nanofluids by implementing an artificial neural network (ANN) using experimental data on viscosity, thermal conductivity, and specific heat. The results based on the ANN model consent with the experimental results in agreement with the different evaluation criteria. Also, a neural network model was developed for estimating the thermophysical properties of magnetic nanofluids and using material informatics to study functional materials. Determining the thermal conductivity (k_{nf}) of oxide of tungsten (WO_3)-MWCNTs/hybrid engine oil, through an Artificial Neural Network (ANN) were presented by Soltani *et al*.[32] The experiments were conducted at a volume fraction of nanoparticles $\varphi = 0.05$ to $\varphi = 0.6\%$, as well as a temperature range of $T = 20°C–60\ °C$. The ANN was then used to estimate the k_{nf}, and the optimum neuron number was 7. Results exhibited that the absolute error values of the ANN method in many points are zero. Also, the ANN had smaller error values compared to the correlation method.

Because of the high effect of thermal conductivity and viscosity on the convection heat transfer coefficient, the required power for pumping, and heat transfer rate, an artificial neural network (ANN) was implemented to predict the mentioned parameters in nanofluids more accurately.

Table 2

Comparing the predicted values of dynamic viscosity of γ-Al_2O_3/water nanofluids using different models

Model&Correlation	μ(kg/m·s)	Condition
Einstein[14]	0.0005623	valid for volume fractions of less than 1%
Brinkman[17]	0.0005854	valid for volume fractions of less than 4%
Batchelor[18]	0.0005915	considered the effect due to the Brownian motion of particles for an isotropic suspension of rigid and spherical particles
Maiga[19]	0.001331	Al_2O_3-water and Al_2O_3-EG nanofluids
Ho[15]	0.001672	valid for Al_2O_3-water nanofluids, d_p= 33 nm $\Phi \leq 4\%$
Williams[16]	0.0403	γ-Al_2O_3/water nanofluid

Table 3

Comparing the predicted values of thermal conductivity of γ-Al_2O_3/water nanofluids using different models

Model &Correlation	k (W/m·K)	Condition
Maxwel[14]	0.866	spherical particles – $\Phi \leq 1\%$
Bruggeman[7]	1.082	considering the interactions between spherical particles
Hamilton and Crosser[5]	0.866	developing the Maxwell model by adding a shape factor
Yu and Choi[8]	1.1068	liquid nanolayer
Xue *et al.*[11]	1.115	nanosuspensions containing carbon nanotubes (CNTs)
Maiga[12]	0.868	Al_2O_3/water nanofluid, d_p= 28 nm
Khanafer and Vafai[14]	1.551	CuO/water – Al_2O_3/water nanofluids, d_p = 13–80 nm
Williams *et al.*[16]	0.953	γ-Al_2O_3/water nanofluid
Ho *et al.*[15]	0.979	Al_2O_3/water nanofluid, d_p= 33 nm – ($\Phi \leq 4\%$)

Principles of artificial neural network

Artificial neural networks (ANNs), usually simply called neural networks (NNs) or, more simply yet, neural nets,[33] are computing systems inspired by the biological neural networks that constitute animal brains.[34] An ANN is based on a collection of connected units or nodes called artificial neurons, which loosely model the neurons in a biological brain. Each connection, like the synapses in a biological brain, can transmit a signal to other neurons. An artificial neuron receives signals then processes them and can signal neurons connected to it. The "signal" at a connection is a real number, and the output of each neuron is computed by some non-linear function of the sum of its inputs. The connections are called edges. Neurons and edges typically have a weight that adjusts as learning proceeds. The weight increases or decreases the strength of the signal at a connection. Neurons may have a

threshold such that a signal is sent only if the aggregate signal crosses that threshold. Typically, neurons are aggregated into layers. Different layers may perform different transformations on their inputs. Signals travel from the first layer (the input layer), to the last layer (the output layer), possibly after traversing the layers multiple times.

ANNs are robust mathematical instruments able to model the nonlinear and complex functions by mimicking the behavior of the biological neural network. The multi-layer perception (MLP) network is the most utilized and basic ANN to solve a regression problem. MLP networks are a powerful tool for providing non-linear correlations. One input layer, one output layer, and at least one hidden layer are included in this type of network. Each layer completely is linked to the next one consisting of some highly parallel and interconnected computational elements known as neurons or nodes. In modeling ANNs, an artificial neuron is a simple processing factor determined by a bias (*b*), weights (*w*), and a transfer/activation function (*f*). Utilizing a random number generator, the weight values are adjusted. Multiplying the inputs for each neuron by the weight values, the outcomes are introduced with the bias value and with each other. The neuron output is then extracted via an appropriate transfer function.

The procedure of discovering appropriate biases and weights for learning the relationship between input and output (target) variables is known as "training". A training algorithm is used by the MLP network data for modifying the neurons' weights based on the error between the actual and expected values until learning the best relationship by the ANN between outputs and inputs. The most prevalent algorithm to train the MLP network is feedforward backpropagation (FFBP). In the feedforward stage of this algorithm, information processing is transmitted from the input layer to the output layer. Over the backward procedure, the errors between the actual and predicted data are determined and then transmitted back to the input layer for adjusting the biases and weights.[35] Such a training procedure includes a step at a time for minimizing the error between the output determined by the actual one and the network.

Overtraining or over fitting is one of the major drawbacks of ANN training, in which the created ANN system produces only good estimation for identified data set and does not offer a rational predicting the novel data set.[36] Using an early termination criterion, it is possible to inhibit overfitting and enhance the network's generalization ability.[37] In such a technique, the data are classified randomly into 3 sub-sets of training, testing, and validation. The training set is used for training the network (setting the biases and weights values) and the validation set is employed for generalizing the developed network and ensuring the accuracy over the training procedure. The network training process is stopped when the validation set error exceeds an assigned threshold; however, further training is done for minimizing the training set error.[38] Stopping the training of the network, the testing set is used for examining the network's ultimate behavior.

RESULTS AND DISCUSSION

Artificial neural network modeling

In this modeling, a feedforward neural network is run in which connections between the nodes do not form a loop. For this purpose, three sets of matrices were defined and the numerical values of each set were determined:

1) A set of weight matrices; In this investigation, because of using only one hidden layer, two matrices were defined.

2) A single matrix that holds the numerical values of *S*, which was the coefficient that describes the steepness of the activating function.

3) A single matrix that holds the numerical values of biases, which would add more flexibility to the neural network.

A genetic algorithm (GA) was implemented to train and determine the numerical values of the mentioned matrices elements. In this study, there were four inputs including 1) nanoparticle size, d_p(nm); 2) nanoparticle volume fraction (φ); 3) temperature T (°C); and 4) molecular weight nanoparticle M_w (g/mol).

This neural network had also four outputs for nanofluids: 1) density ρ (kg/m^3); 2) viscosity μ, (Pa·s); 3) specific heat C_p (J/kg·K); and 4) thermal conductivity k (W/m·K).

A tangent hyperbolic function was selected as the transfer function:

$$Y = \tanh(S \cdot X + B) \tag{26}$$

where *Y*, *S*, *X*, and *B* are output, steepness, input, and bias, respectively. The neural network topography includes matrices numerical values presented in Fig. 2.

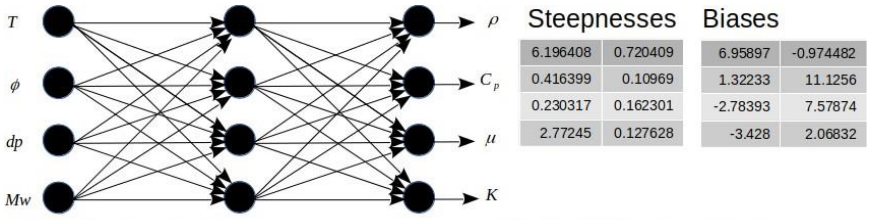

Steepnesses

6.196408	0.720409
0.416399	0.10969
0.230317	0.162301
2.77245	0.127628

Biases

6.95897	-0.974482
1.32233	11.1256
-2.78393	7.57874
-3.428	2.06832

Weight input → hidden

4.28556	0.00000	0.00000	0.466168
0.00000	2.12996	0.23885	0.074212
-6.88325	0.356631	-0.33245	3.72407
1.2624	0.303597	4.83108	0.00000

Weight hidden → output

-0.429645	1.42642	0.000000	-0.213016
-1.91754	-4.94439	0.000000	12.5868
-9.43084	0.487114	0.8283220	1.5629
0.000000	3.08302	-3.25366	0.835897

Fig. 2 – Detailed decryption of the ANN.

The entire data were randomly grouped into three bathes: 60% for training the network, 20% for cross-validating, and 20% remaining for testing purposes. The data were normalized to the range (–1, +1) before importing them to the network. Many topographies were tried in a computer program written in C ++ language. It was found that the architecture (4, 4, 4) had the least cross-validation error. Numbers in the curly brace define the numbers of input, neurons in the concealed (hidden) layer, and outputs, respectively. Larger topographies with more neurons in the hidden layer or more hidden layers were found to overfit the data. Also, they were associated with higher validation and test data set errors. The training, cross-validating, and testing errors were found equal to 1%, 2%, and 1%, respectively.

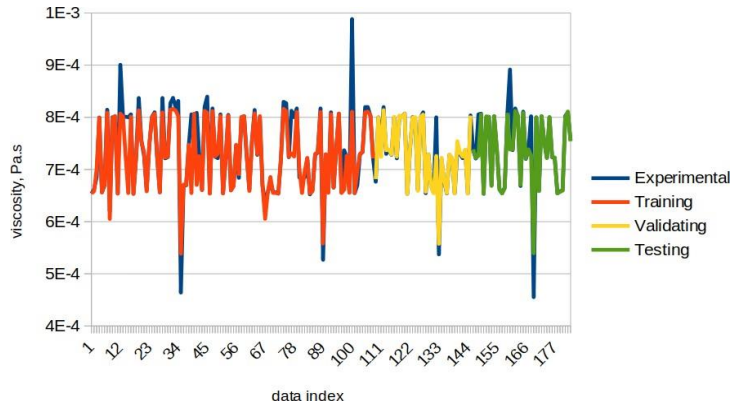

Fig. 3 – A typical comparison between the experimental and predicted viscosity values.

The number of chromosomes and iteration was selected equal to 100 and 200, respectively. A dual Intel Xeon 2600 with a total of 16 cores and 31 threads were computed in a multi-threading manner. Figures 3 and 4 compares the experimental and expected viscosity and thermal conductivity values.

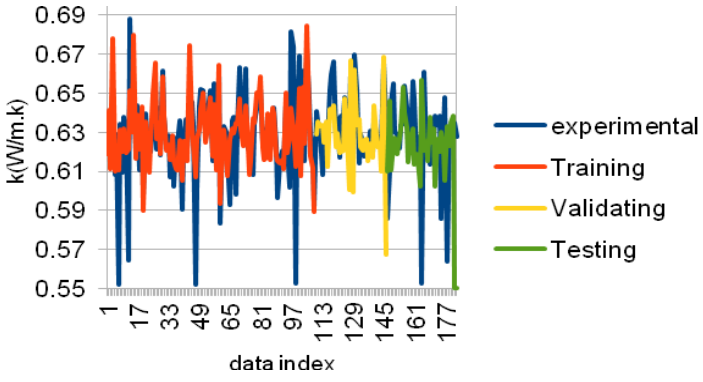

Fig. 4 – A typical comparison between the experimental and predicted thermal conductivity values.

Sensitivity analysis

After the network training and testing were completed, the sensitivity analysis was conducted to define the effect of each input parameter and constant condition. In Figs. 5, 6, and 7, the nanofluid viscosity was predicted as a function of nanofluid volume fraction at various nanoparticle molecular weights. Results show that at a temperature of 30 ºC and particle size of 10 nm, nanofluid viscosity has a maximum at around 1.5 vol.%, while at 45 ºC and particle size of 31nm, nanofluid viscosity almost monotonically increases with concentration. Interestingly, at 65 ºC and particle size of 40 nm, nanofluid viscosity has a minimum of about 1.25 vol.%. Possible mechanisms for change in nanofluid's viscosity may involve hydrodynamic interactions between surface particles, an increase in surface particles, increased energy dissipation rate, integrated impacts of particle aggregation and electroviscous forces, and the impacts of the electric double layer repulsion.[39]

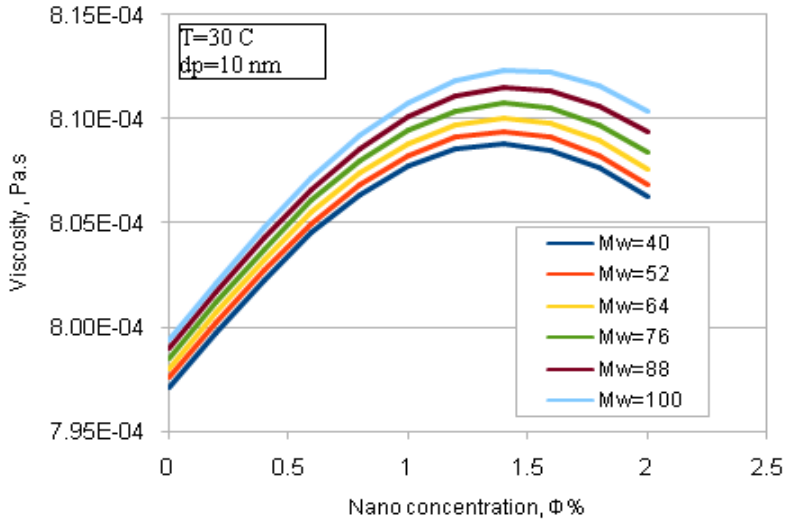

Fig. 5 – A typical prediction of nanofluid viscosity as a function of volume fraction at various nanoparticle molecular weights at a temperature of 30 ºC and particle size of 10 nm.

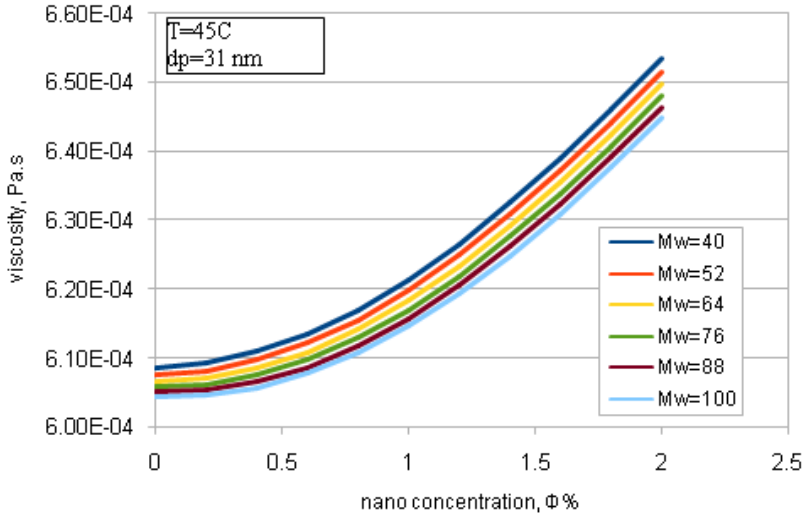

Fig. 6 – A typical prediction of nanofluid viscosity as a function of volume fraction at various nanoparticle molecular weights at 45 ºC and particle size of 31nm.

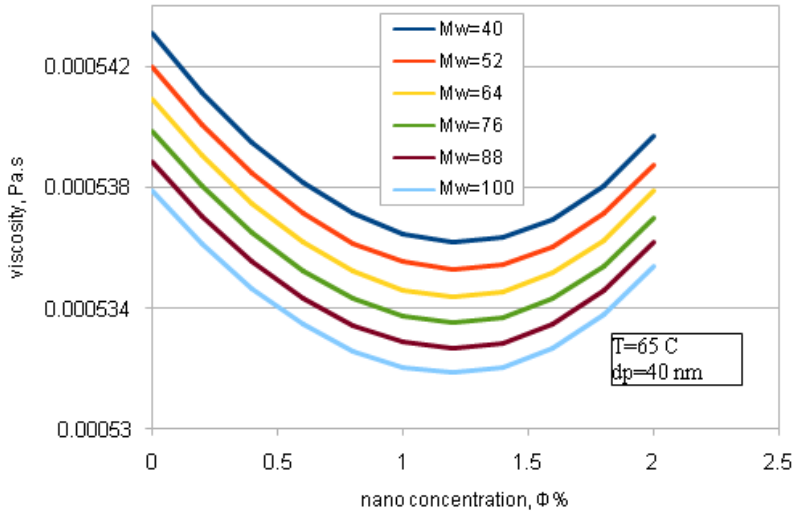

Fig. 7 – A typical prediction of nanofluid viscosity as a function of volume fraction at various nanoparticle molecular weights at 65 ºC and particle size of 40 nm.

Figure 8 illustrates a typical estimation of nanofluid viscosity as a function of nanoparticle size at different nanoparticle molecular weights at 30 ºC and volume fraction of 0.2%. Other fractions and temperatures present more or less similar trends. Larger particle size and higher molecular weight of nanoparticle increase the viscosity of nanofluid because of higher inertia and consequently lower magnitude of Brownian motions.

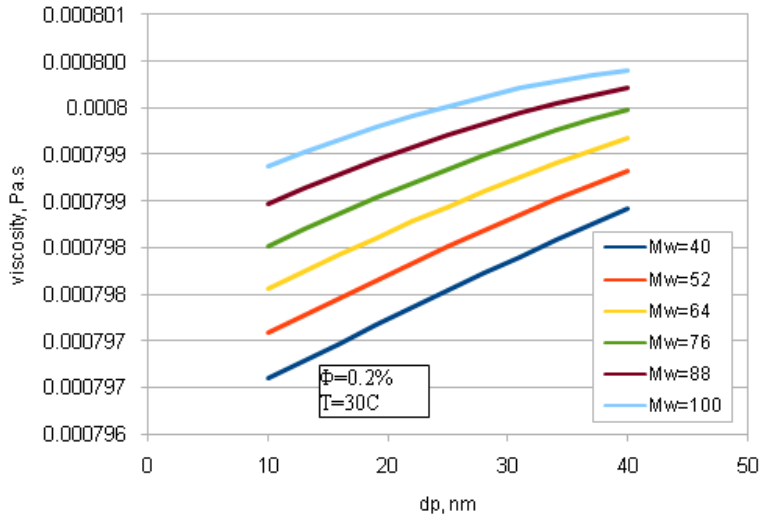

Fig. 8 – A typical prediction of nanofluid viscosity as a function of nanoparticle size at various nanoparticle molecular weights at 30 ºC and volume fraction of 0.2%.

Figures 9 and 10 depict the prediction of nanofluid thermal conductivity as a function of volume fraction at various nanoparticle molecular weights at 10 ºC and particle size of 10 nm also at 65 ºC and particle size of 40 nm. The lower molecular weight yields a higher thermal conductivity at any constant concentration at temperatures of 10 ºC and nanoparticle sizes of 10 nm. However, at 65 ºC and nanoparticle size of 40 nm, the molecular weight has a negligible impact on thermal conductivity.

Conclusions on the effect of molecular weight on thermal conductivity require further studies. Nanofluids' thermal conductivity can be explained by several reasons and mechanisms; *e.g.*, the mixing impacts of particles near the wall, particle

migration, Brownian motion of particles, and reduced boundary layer thickness.[40] The response to the question "which is the leading heat transport mechanism in charge of the thermal conductivity improvement in nanofluids" is still a matter of debate.

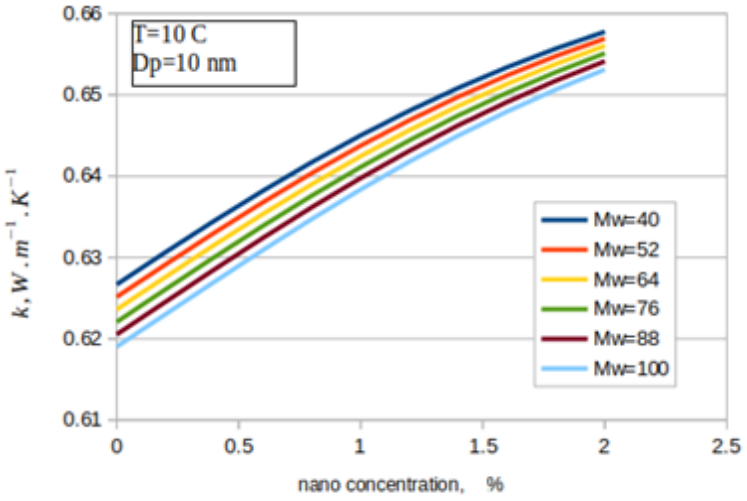

Fig. 9 – A typical prediction of nanofluid thermal conductivity as a function of volume fraction at various nanoparticle molecular weights at 10 ºC and particle size of 10 nm.

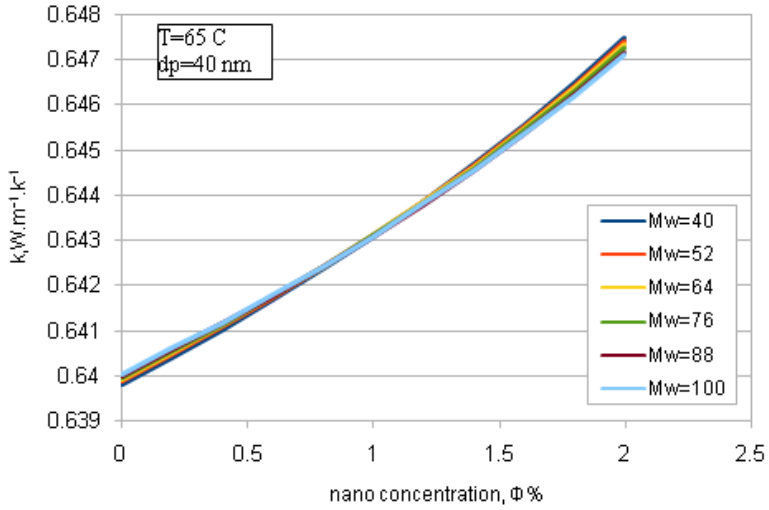

Fig. 10 – A typical prediction of nanofluid thermal conductivity as a function of volume fraction at various nanoparticle molecular weights at 65 ºC and particle size of 40 nm.

CONCLUSION

In this study, based on 184 independent data points of thermophysical properties from literature, an artificial neural network (ANN) was implemented. The data include various metal oxides comprising Al_2O_3, SiO_2, TiO_2, Fe_2O_3, MgO, and CuO at a temperature range of 30–65 ºC, diameter range of 10–50 nm, and volume fraction range of 0.004–2%. The ANN was implemented and the parameters of thermal conductivity and viscosity were correlated to nanofluid concentration, particle size, temperature, and molecular weight. The major conclusions of this work are outlined as follows:

Existing correlations and models fail to predict thermophsical properties with acceptable accuracy.

Topography of (4, 4, 4) provides least cross validating error.

At volume fraction (nanofluid) of about 1.4%, the dynamic viscosity is maximum at 10 ^{0}C and 30 nm particle diameter. In average, by increasing 10 g/gmol nanofluid molecular weight, viscosity increases by 0.8%.

At 45^{0}C and 31 nm particle diameter, nanofluid viscosity monotonically increases by increasing nanoparticle concentration. In In average, by increasing 10 g/mol nanofluid molecular weight, viscosity decreases by 1.5%.

At 65 ^{0}C and 40 nm particle diameter and volume fraction of nanofluid of 1.25%, viscosity has a minimum value. In average, by increasing 10 g/gmol nanofluid molecular weight, viscosity decreases by 0.34%.

Thermal conductivity of nanofluid monotonically increases by nanoparticle concentration with tangent of 0.03 W/m·K by each vol. 1% of nanoparticle concentration.

Nomenclature list of symbols

n – shape factor
k_B – Boltzmann constant
d_p – nanoparticle diameter
ANN – artificial neural network
T – temperature

Greek symbols

Φ – volume concentration
μ_{nf} – viscosity
ρ – density
ø – sphericity
ã – nanolayer thickness

Subscripts

ave – average
f – base fluid
p – nanoparticle
nf – nanofluid

REFERENCES

1. R. Taylor, S. Coulombe, T. Otanicar, P. Phelan, A. Gunawan, W. Lv, G. Rosengarten, R. Prasher and H. Tyagi, *J. Appl. Phys.*, **2013**, *113*, 011301.
2. a) S. U. S. Choi, in Argonne National Lab.(ANL), Argonne, IL (United States) , **1995**, p. 99; b) P. Keblinski, S. Phillpot, S. Choi and J. Eastman, *Int. J. Heat Mass Transfer*, **2002**, *45*, 855; c) X. Wang, X. Xu and S. U. Choi, *J. Thermophys Heat Transfer*, **1999**, *13*, 474.
3. a) W. Azmi, K. Sharma, R. Mamat, G. Najafi and M. Mohamad, *Renewable and Sustainable Energy Reviews*, **2016**, *53*, 1046; b) W. J. Tseng and K.-C. Lin, *Mater. Sci. Engineer.: A*, **2003**, *355*, 186; c) I. Mahbubul, R. Saidur and M. Amalina, *Int. J. Heat Mass Transfer*, **2012**, *55*, 874; d) M. Corcione, *Energy Convers. Manage.*, **2011**, *52*, 789; e) S. Murshed, K. Leong and C. Yang, *Appl. Therm. Eng.*, **2008**, *28*, 2109.
4. J. C. Maxwell, *A Treatise on Electricity and Magnetism*, Clarendon Press, Oxford, UK, 1881.
5. R. L. Hamilton and O. Crosser, *Ind. Engineer. Chem. Fundamentals*, **1962**, *1*, 187.
6. E. J. Wasp, J. P. Kenny and R. L. Gandhi, *Ser. Bulk Mater. Handl.(United States)* **1977**, *1*,4.
7. V. D. Bruggeman, *Annalen der physik*, **1935**, *416*, 636.
8. W. Yu and S. Choi, *J. Nanopart. Res.*, **2003**, *5*, 167.
9. Y. Xuan, Q. Li and W. Hu, *AlChE J.*, **2003**, *49*, 1038.
10. J. Koo and C. Kleinstreuer, *J. Nanopart. Res.*, **2004**, *6*, 577.
11. Q. Xue, *Physica B: Condensed. Matter*., **2005**, *368*, 302.
12. S. E. B. Maïga, S. J. Palm, C. T. Nguyen, G. Roy and N. Galanis, *Int. J. Heat Fluid Flow.*, **2005**, *26*, 530, DOI: http://dx.doi.org/10.1016/j.ijheatfluidflow.2005.02.004.
13. M. Corcione, *Int. J. Therm. Sci.*, **2010**, *49*, 1536.
14. K. Khanafer and K. Vafai, *Int. J. Heat Mass Transfer*, **2011**, *54*, 4410.
15. C. Ho, W. Liu, Y. Chang and C. Lin, *Int. J. Therm. Sci.*, **2010**, *49*, 1345.
16. W. Williams, J. Buongiorno and L.-W. Hu, *J. Heat Transf.*, **2008**, *130*, 042412.
17. H. Birkman, *J. Chem. Phys.*, **1952**, *20*, 571.
18. G. Batchelor, *J. Fluid Mech.*, **1977**, *83*, 97.
19. S. El Bécaye Maïga, C. Tam Nguyen, N. Galanis, G. Roy, T. Maré and M. Coqueux, *Int. J. Numerical Methods for Heat & Fluid Flow*, **2006**, *16*, 275.
20. R. S. Vajjha, University of Alaska Fairbanks, PhD Thessis: Experimental and computational studies of nanofluids, **2014**.
21. O. Mahian, A. Kianifar, C. Kleinstreuer, A.-N. Moh'd A, I. Pop, A. Z. Sahin and S. Wongwises, *Int. J. Heat Mass Transfer*, **2013**, *65*, 514.
22. a) B. Raei and S. M. Peyghambarzadeh, *J. Chem. Petroleum Engineer.*, **2021**, *55*, 117, DOI: 10.22059/jchpe.2021.307767.1323; b) B. Raei and S. M. Peyghambarzadeh, *J. Chem. Petroleum Engineer.*, **2019**, *53*, 25; c) B. Raei, F. Shahraki, M. Jamialahmadi and S. Peyghambarzadeh, *J. Therm. Anal. Calorim.*, **2017**, *127*, 2561; d) B. Raei, F. Shahraki and S. M. Peyghambarzadeh, *Experim. Heat Transfer*, **2018**, *31*, 68, DOI: 10.1080/08916152.2017.1353557; e) B. Raei, F. Shahraki, M. Jamialahmadi and S. M. Peyghambarzadeh, *Transport Phenomena in Nano and Micro Scales*, **2016**, *5*, 64, DOI: 10.7508/tpnms.2017.01.007; f) B. Raei, S. Peyghambarzadeh and R. S. Asl, *Appl. Therm. Eng.*, **2018**, *144*, 926.
23. H. Kurt and M. Kayfeci, *Applied energy*, **2009**, *86*, 2244.
24. M. M. Papari, F. Yousefi, J. Moghadasi, H. Karimi and A. Campo, *Int. J. Therm. Sci.*, **2011**, *50*, 44.
25. A. Alirezaie, S. Saedodin, M. H. Esfe and S. H. Rostamian, *J. Mol. Liq.*, **2017**, *241*, 173.
26. M. Hojjat, S. G. Etemad, R. Bagheri and J. Thibault, *Int. J. Heat Mass Transfer*, **2011**, *54*, 1017.
27. A. Karimipour, S. Ghasemi, M. H. K. Darvanjooghi and A. Abdollahi, *Int. Commun. Heat Mass*, **2018**, *92*, 90.
28. G. A. Longo, C. Zilio, L. Ortombina and M. Zigliotto, *Int. Commun. Heat Mass*, **2017**, *83*, 8.
29. M. H. Esfe, S. Saedodin, A. Naderi, A. Alirezaie, A. Karimipour, S. Wongwises, M. Goodarzi and M. bin Dahari, *Int. Commun. Heat Mass*, **2015**, *63*, 35.
30. M. Vakili, S. Khosrojerdi, P. Aghajannezhad and M. Yahyaei, *Int. Commun. Heat Mass*, **2017**, *82*, 40.
31. L. Shi, S. Zhang, A. Arshad, Y. Hu, Y. He and Y. Yan, *Renewable and Sustainable Energy Reviews*, **2021**, *149*, 111341.
32. F. Soltani, M. Hajian, D. Toghraie, A. Gheisari, N. Sina and A. A. Alizadeh, *Case Studies in Thermal Engineering*, **2021**, *26*, 101122, DOI: https://doi.org/10.1016/j.csite.2021.101122.
33. L. Hardesty, "Explained: neural networks", *MIT News*, **2017**, *14*.

34. A. Brahme, "Comprehensive biomedical physics", Newnes, 2014.
35. Q. Feng, J. Zhang, X. Zhang and S. Wen, *Fuel Process. Technol.*, **2015**, *129*, 120.
36. H. Sayyad, A. K. Manshad and H. Rostami, *Fuel*, **2014**, *116*, 625.
37. M. Ariana, B. Vaferi and G. Karimi, *Powder Technol.*, **2015**, *278*, 1.
38. S. Jung and S.-D. Kwon, *Appl. Energy*, **2013**, *111*, 778.
39. M. Chandrasekar, S. Suresh and T. Senthilkumar, *Renewable and Sustainable Energy Reviews*, **2012**, *16*, 3917.
40. a) D. Kim, Y. Kwon, Y. Cho, C. Li, S. Cheong, Y. Hwang, J. Lee, D. Hong and S. Moon, *Curr. Appl. Phys.*, **2009**, *9*, e119, DOI: http://dx.doi.org/10.1016/j.cap.2008.12.047; b) W. Duangthongsuk and S. Wongwises, *Int. J. Heat Mass Transfer*, **2010**, *53*, 334, DOI: http://dx.doi.org/10.1016/j.ijheatmasstransfer.2009.09.024.